

Metagenome-Assembled Genomes of *Komagataeibacter* from Kombucha Exposed to Mars-Like Conditions Reveal the Secrets in Tolerating Extraterrestrial Stresses

Imchang Lee^{1,2}, Olga Podolich³, Bertram Brenig⁴, Sandeep Tiwari⁵, Vasco Azevedo⁵, Daniel Santana de Carvalho⁶, Ana Paula Trovatti Uetanabaro⁶, Aristóteles Góes-Neto⁶, Khalid J. Alzahrani⁷, Oleg Reva⁸, Natalia Kozyrovska³, Jean-Pierre de Vera⁹, Debmalya Barh^{5,10*}, and Bong-Soo Kim^{1,11*}

¹Department of Life Science, Multidisciplinary Genome Institute, Hallym University, Chuncheon 24252, Republic of Korea

²Institute for Liver and Digestive Diseases, Hallym University, Chuncheon, Republic of Korea

³Institute of Molecular Biology and Genetics of NASU, Kyiv 03143, Ukraine

⁴Institute of Veterinary Medicine, Burckhardtweg, University of Göttingen, Göttingen 37073, Germany

⁵Departamento de Genética, Ecologia e Evolução, Instituto de Ciências Biológicas, Universidade Federal de Minas Gerais, Belo Horizonte, Minas Gerais 6627, Brazil

⁶Molecular and Computational Biology of Fungi Laboratory, Department of Microbiology, Institute of Biological Sciences, Federal University of Minas Gerais, Belo Horizonte 6627, Brazil

⁷Department of Clinical Laboratories Sciences, College of Applied Medical Sciences, Taif University, Taif 21944, Saudi Arabia

⁸Centre for Bioinformatics and Computational Biology, Department of Biochemistry, Genetics and Microbiology, University of Pretoria, Pretoria 0028, South Africa

⁹Microgravity User Support Center (MUSC), German Aerospace Center (DLR), Cologne 51147, Germany

¹⁰Institute of Integrative Omics and Applied Biotechnology (IIIOAB), Nonakuri, Purba Medinipur, WB, 721172, India

¹¹The Korean Institute of Nutrition, Hallym University, Chuncheon 24252, Republic of Korea

Received: April 7, 2022

Accepted: July 5, 2022

First published online:
July 7, 2022

*Corresponding authors
D. Barh
E-mail: dr.barh@gmail.com
B.-S. Kim
Phone: +82-33-248-2093
Fax: +82-33-256-3420
E-mail: bkim79@hallym.ac.kr

eISSN 1017-7825
eISSN 1738-8872

Copyright © 2022 by the authors.
Licensee KMB. This article is an
open access article distributed
under the terms and conditions
of the Creative Commons
Attribution (CC BY) license.

Kombucha mutualistic community (KMC) is composed by acetic acid bacteria and yeasts, producing fermented tea with health benefits. As part of the BIOlogy and Mars EXperiment (BIOMEX) project, the effect of Mars-like conditions on the KMC was analyzed. Here, we analyzed metagenome-assembled genomes (MAGs) of the *Komagataeibacter*, which is a predominant genus in KMC, to understand their roles in the KMC after exposure to Mars-like conditions (outside the International Space Station) based on functional genetic elements. We constructed three MAGs: *K. hansenii*, *K. rhaeticus*, and *K. oboediens*. Our results showed that (i) *K. oboediens* MAG functionally more complex than *K. hansenii*, (ii) *K. hansenii* is a keystone in KMCs with specific functional features to tolerate extreme stress, and (iii) genes related to the PPDK, betaine biosynthesis, polyamines biosynthesis, sulfate-sulfur assimilation pathway as well as type II toxin-antitoxin (TA) system, quorum sensing (QS) system, and cellulose production could play important roles in the resilience of KMC after exposure to Mars-like stress. Our findings show the potential mechanisms through which *Komagataeibacter* tolerates the extraterrestrial stress and will help to understand minimal microbial composition of KMC for space travelers.

Keywords: Kombucha, *Komagataeibacter*, metagenome assembled genome, mars-like condition, whole metagenome

Introduction

Kombucha is one of the most popular healthy beneficial beverage consumed in all over the world [1, 2]. The effects of Kombucha and its ingredients on health has been reported in several studies [1-3]. Recently, the microbiome of Kombucha mutualistic community (KMC) has been largely studied to understand the microbial roles in the beneficial effects of Kombucha. Although the microbial composition is varied among different KMCs, dominant members (*Brettanomyces*, *Pichia*, *Saccharomyces*, *Schizosaccharomyces* and *Zygosaccharomyces* as yeast

members, and *Acetobacter*, *Lactobacillus*, *Leuconostoc*, *Bifidobacterium*, and *Komagataeibacter* as bacterial members) were the most common representatives [2-5]. *Komagataeibacter* species have been focused on as dominant bacteria that produce cellulose, gluconic, and glucuronic acid by fermentation in KMCs [6, 7]. The microbiome, which consists of various microbes, is a dynamic ecosystem that shares genetic elements with each other and responds to their habitat's changes. Among the members, substantially essential organisms for controlling the function and maintenance of the microbiome are called keystone taxa and dominant taxa [8]. Therefore, analysis of the keystone taxa is important to understand the shift of the microbiome and to determine the minimal composition of the microbes in a stressed environment.

In the BIOMEX (Biology and Mars Experiment) project, Kombucha samples were used as a material to understand the influence of exposure to spaceflight and Mars-like conditions on microbiome of Kombucha. The composition of microbiome in KMCs and the effect of long-term exposure to a harsh stressful environment of Martian conditions on dried and partially mineralized cellulose-based KMC biofilms in low Earth orbit were analyzed in our previous studies [9, 10]. In the studies, *Komagataeibacter* was determined as the dominant genus in KMCs exposed to Mars-like conditions, and the cellulose-based biofilm produced by genus *Komagataeibacter* was key material to protect cells from germicidal environments like UV and dried state which were generated Mars-like conditions. Although the microbiome and the importance of *Komagataeibacter* in KMCs exposed to harsh conditions were reported, genetic characteristics of *Komagataeibacter* in KMCs according to exposure conditions by using metagenome-assembled genome (MAG) analysis is not yet done to understand the genomic functionality in extra-terrestrial conditions.

In this study, we reconstructed and analyzed the high-quality MAGs in KMCs exposed to Mars-like conditions outside the International Space Station (ISS) to understand the role of *Komagataeibacter* through the lens of its MAG in survival and to define how the *Komagataeibacter* retains its dominance in KMC under stressful Martian conditions.

Materials and Methods

Samples, Space Exposure Conditions, and Metagenome Sequencing

Experimental conditions for exposure, reactivation, and readaptation of KMC samples and laboratory references were described in our previous study [10]. Briefly, dried KMC pellicles from collection of Institute of Molecular Biology and Genetics (IMBG, Ukraine) were exposed to Mars-like conditions in the three-layer sample carrier on the EXPOSE-R2 facility outside the ISS (Fig. 1). Samples were exposed to UV (> 200 nm), cosmic ionizing radiation, and other fluencies during 2.5-year (18 months outside and 7 months inside the station). Returned KMC pellicles from the ISS were cultured in black tea with white sugar (BTS) medium during 2 weeks for reactivation, and reactivated samples were sub-cultured in BTS medium during 2.5-year for readaptation. Analyzed KMC samples consist of nine samples including one initial KMC sample (KMC_5), three post-flight reactivated samples (KMC_1b, KMC_2b, and KMC_3b) exposed on top, middle, and bottom levels of the carrier, and three readadapted samples (KMC_1c, KMC_2c, and KMC_3c). The top-layer sample was exposed to UV and the samples of middle and bottom layer were maintained unlighted and UV-protected condition during the

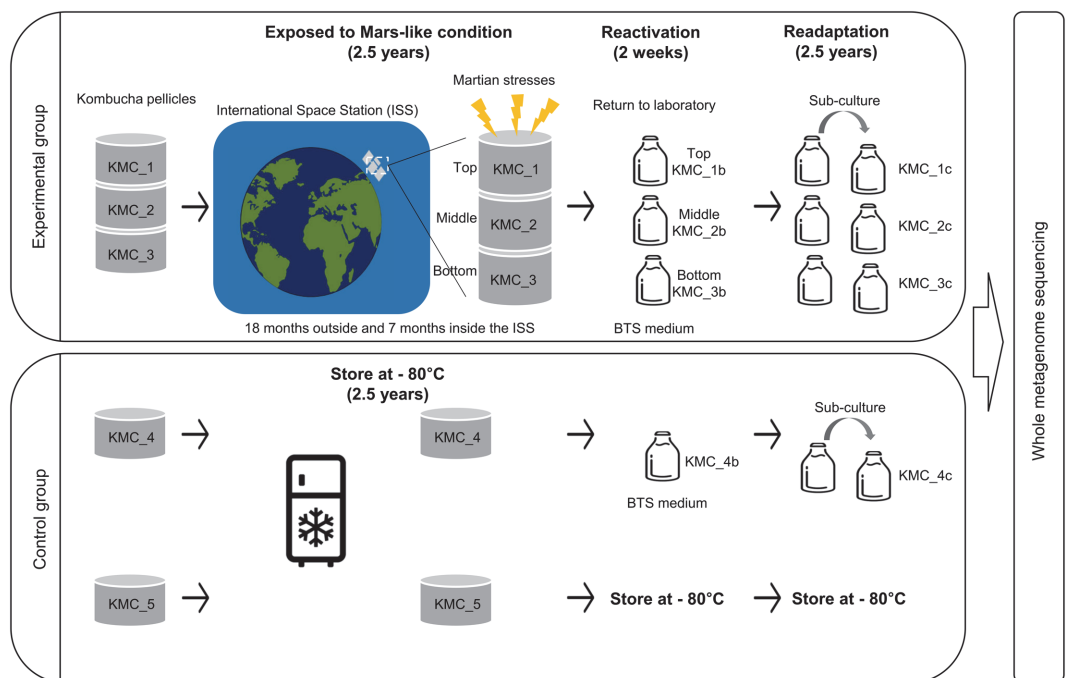


Fig. 1. Summary of experimental schemes in this study.

exposure period. In parallel, laboratory-kept controls, KMC_4b (reactivated along with the returned from the ISS) and KMC_4c (cultured for 2.5-year with KMC_4b) were used as ground-based references. After reactivation, the aliquots of post-flight samples and control samples (laboratory kept sample: KMC_4b and the initial KMC ecotype: KMC_5) were stored at -80°C. The metagenomic DNA extraction and whole metagenome sequencing for all the samples were performed as described in our previous study [9]. The shotgun metagenome sequences were obtained from Illumina HiSeq 2500 (150-bp paired ends).

Analysis of Functional Gene Profiles in Whole Metagenome Sequences Based on Short-Reads

Functional gene profiles in KMC samples were analyzed by using the HMP Unified Metabolic Analysis Network (HUMAN 3.0) tool [11]. The differences of profiles between the samples were analyzed in the nonmetric multidimensional scaling (NMDS) plot [12] based on the Bray-Curtis dissimilarity matrix [13]. Fifty iterations were performed and the resulting ordination that had the lowest stress was used for data visualization. The monoMDS function implemented by the vegan package of R was used for MDS [14]. Taxonomic identification for functional genes and the conversion of functional gene features to KEGG Orthology (KO) were obtained from the HUMAN. The relative abundance of species was normalized with copies per million (CPM) and unmapped reads were excluded for comparison among samples. The changed KOs in each KMC sample compared to initial KMC sample (KMC_5) were analyzed by heatmap plot.

Reconstruction of the MAGs

The co-assembly of the quality-filtered reads was performed using MEGAHIT ver. 1.2.9 [15], and the contigs shorter than 1 kb were discarded. After the co-assembly process, the rest of the sequencing reads were mapped to the assembled contigs using Bowtie2 ver. 2.4.1 [16]. The co-assembled and mapped reads were binned based on the single-copy core gene (SCG) set of Kaiju ver. 1.6.2 [17] using Anvi'o ver. 6.2 [18]. The Anvi-refine inherent in the Anvi'o was used to identify pairs of bins. The completeness and contamination of the reconstructed bins were estimated using CheckM ver. 1.1.3 [19]. MAGs with an estimated completeness > 90% and contamination < 5% were used for further analyses.

Classification of MAGs

The reconstructed MAGs were initially classified with SCG of Kaiju program and the detected SCG were identified using BLASTP program [20] with the National Center for Biotechnology Information (NCBI)-nr database [21]. For accurate classification of MAGs, the genomic distances between the completed genome sequences of closest strains predicted based on BLASTP results and obtained MAGs were calculated using OrthoANI tool [22]. The genomic nucleotide variation-based phylogenetic trees were used for inferring the evolutionary relationship between MAGs and a given reference type strains using PhaME tool [23]. Bootstrap analysis was performed by resampling 100 times the entire set, and the bootstrap values were displayed on the maximum likelihood phylogeny tree. In order to reduce bias during the reconstruction of the MAGs, only accurately classified MAGs among the reconstructed bins were used for further analysis.

Assignment of Functional Genetic Elements in MAGs

In order to identify functional genes in MAGs, gene contents in each MAG were assigned at module-level using the GhostKoala ver. 2.2 with default options in the KEGG database ver. 96.0 [24]. The information of the functional operon in the MAGs was obtained from the annotated data generated by using the Prokka program [25]. The sequence data of the reconstructed *Komagataeibacter* MAGs in this study were deposited in the NCBI GenBank database under the accession numbers of GCA_016785065.1, GCA_016785115.1, and GCA_016785145.1.

Results

Comparison of Functional Gene Profiles Based on Short-Reads among KMCs Samples

The differences of functional gene profiles among KMC samples were analyzed by means of an analysis of similarities (ANOSIM) based on the rank-order Bray-Curtis distance (Fig. 2A). Functional genes of microbiome in samples of a control group (KMC_4b, KMC_4c, KMC_5), a post-flight reactivated group (KMC_1b, KMC_2b, KMC_3b), and a readapted group (KMC_1c, KMC_2c, KMC_3c) were significantly different ($p = 0.011$). Two species of *K. hansenii* and *K. oboediens* were found to be dominant members in all samples, and the relative abundances of these two species were higher in the top-layer samples (95.22% of *K. hansenii* in KMC_1b and 91.89% of *K. oboediens* in KMC_1c) than other samples (Fig. 2B). Functional genes of unclassified taxa were relative higher in laboratory-kept samples (mean value of 63.95%) than KMC samples after exposure Mars-like condition. *K. hansenii* was dominant in laboratory-kept samples (KMC_4b, KMC_4c, and KMC_5) and top-layer of post-flight reactivated sample (KMC_1b). The relative abundances of *K. oboediens* were increased in middle- and bottom-layers of reactivated samples (KMC_2b and KMC_3b) and all layers of readapted samples (KMC_1c, KMC_2c, and KMC_3c). The changed KOs compared to the initial sample (KMC_5) were different between top-layer samples (KMC_1) and other samples (Fig. 2C). The relative abundances of KOs were decreased more in reactivated top-layer sample (KMC_1b) than other samples, whereas their abundances were increased more in readapted top-layer sample (KMC_1c). Most of them were related to biosynthesis of nucleotides and amino acids.

Reconstruction and Identification of the MAGs: *K. hansenii*, *K. rhaeticus*, and *K. oboediens*

A total of 497,559,912 reads were co-assembled resulting in 7,303 metagenomic contigs with a mean length of > 65,241 kb. The contigs with short length (< 1,000 bp) were removed from 7,303 contigs, and the resultant 1,435

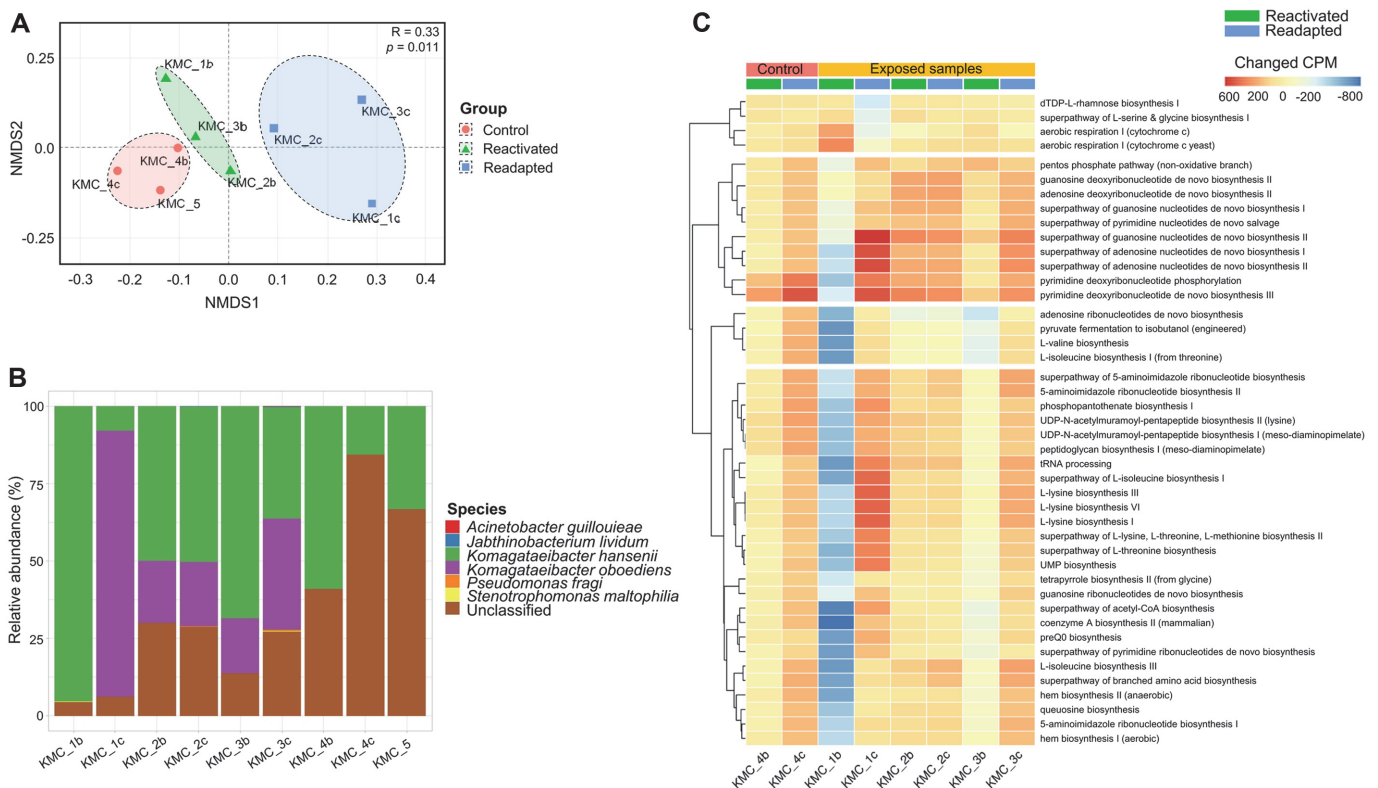


Fig. 2. Comparison of functional profiles among KMC samples. (A) The difference of functional features in microbiome of KMCs was analyzed by NMDS plot based on Bray-Curtis dissimilarity. Red indicates control group, green indicates post-flight group, and blue indicates readapted post-flight group. (B) The relative abundances of species identified by functional genes were compared among KMC samples. The relative abundance of the taxa was normalized using copies per million (CPM), and unmapped reads were excluded in analysis. (C) The changed KEEG Ortholog (KO) in KMC samples compared to initial reference sample (KMC_5) were analyzed by heatmap.

contigs were used for the binning process. Six bins were retrieved after binning, and 2 bins (bin004 and 005) were removed by quality check of completeness (> 90%) and contamination (< 5%) (Fig. 3). These two bins that were removed, bin004 (89.16% completeness) and bin005 (83.13% completeness), were predicted as *Pichia* (a yeast genus) based on the SCG set of Kaiju. Although bin006 was predicted as *Pseudomonas* with high quality (100% completeness and 1.41% contamination), it was not accurately classified in a detailed analysis to delineate species using taxonomical indices including average nucleotide identity (ANI) value and 16S rRNA gene similarity. Thus, we had excluded bin006 from analysis to reduce misunderstanding by potential biases during MAG reconstruction [26]. As a result, three bins (bin001, bin002, and bin003) were retrieved from all the KMC samples and were predicted as *Komagataeibacter* (bin001 and 003) and Family *Acetobacteraceae* (bin002) by the SCG set of Kaiju. The bin001, bin002, and bin003 were named as kmcMAG001, kmcMAG002, and kmcMAG003 for further analyses.

For accurate classification of these three bins, a phylogenomic analysis was performed with the closest strains. The similarity between MAGs and the genome of the closest strains was calculated by ANI value (Fig. 4A). The ANI value between kmcMAG001 and *K. hansenii* ATCC23769 was 97.40%, and that between kmcMAG002 and *K. rhaeticus* ENS90a1a was 98.89%, and that between kmcMAG003 and *K. oboediens* BPZTR01 was 98.58%. The classification of the MAGs at species-level was determined by genome single nucleotide polymorphism (SNP) tree with the MAGs and the genomes of type strains of the predicted species. As a result, the MAGs were classified as *K. hansenii* (kmcMAG001), *K. rhaeticus* (kmcMAG002), and *K. oboediens* (kmcMAG003) (Fig. 4B). General features of three obtained MAGs were summarized in our previous report [27]. Briefly, genome sizes of the three *Komagataeibacter* MAGs were in a range from 3,326,596 to 4,214,122 bp, and their correspondent GC contents were in a range from 60.14% to 63.35%. The N_{50} values of the MAGs displayed a range of 62,857 to 88,723 bp. Estimated completeness of the kmcMAG001, kmcMAG002, and kmcMAG003 were 94.65%, 99.11%, and 98.77%, respectively, and redundancy (contamination rate) were 4.98%, 1.69%, and 1.49%, respectively.

Comparison of Functional Gene Features among Three *Komagataeibacter* MAGs

The three reconstructed *Komagataeibacter* MAGs were dominant members in all the KMC samples, and they could play as keystone in KMCs. Thus, we compared the gene contents among the three *Komagataeibacter* MAGs (Fig. 5). A total of 59 genetic elements, including 53 completed module-level pathways and six operons were

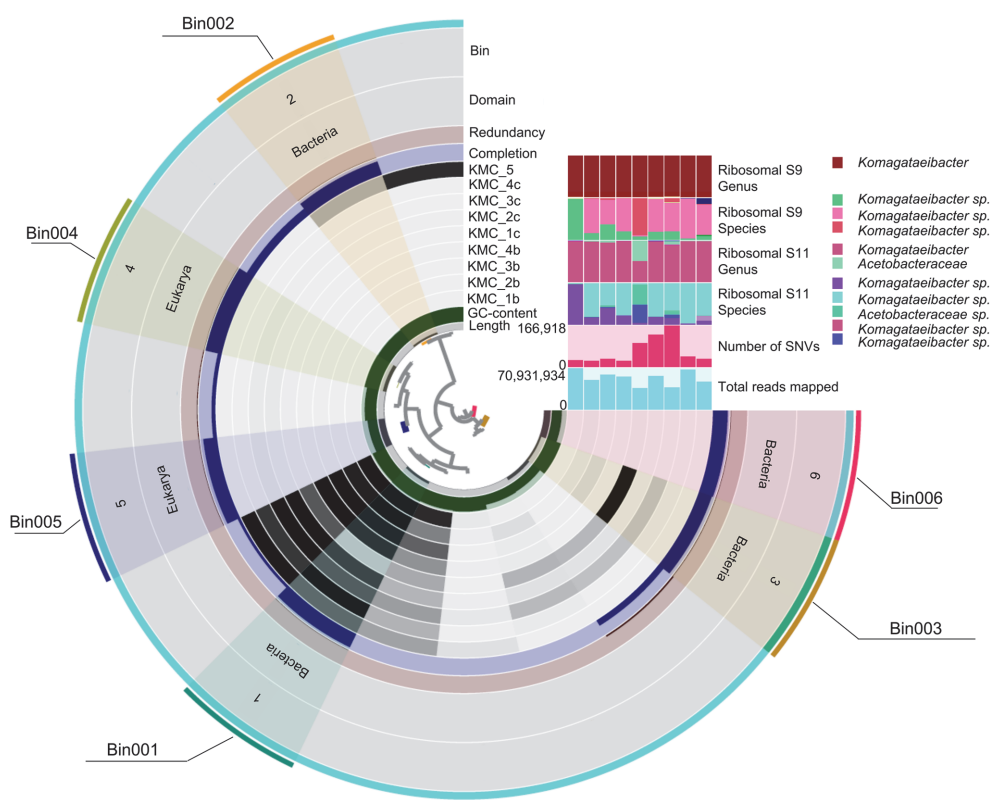


Fig. 3. Comparison of bin results from metagenome sequences using Anvi'o program. Dendrogram shows the distribution and taxonomic identification of each bin based on single-copy core gene (SCG) of Kaiju. The first inner circle showed the length of each SCG, and second circle indicated GC contents (%). The following nine circle layers represented the proportion of contigs in each KMC sample. The next layers showed the completeness, redundancy, and taxonomic information of each bin. The proportion of total mapped reads and the number of single nucleotide variation (SNV) in each KMC samples were compared by 5th and 6th of upper-right bar chart. The relative abundance of taxonomic composition by each marker gene set was compared among KMC samples by 1st to 4th of upper-right bar charts.

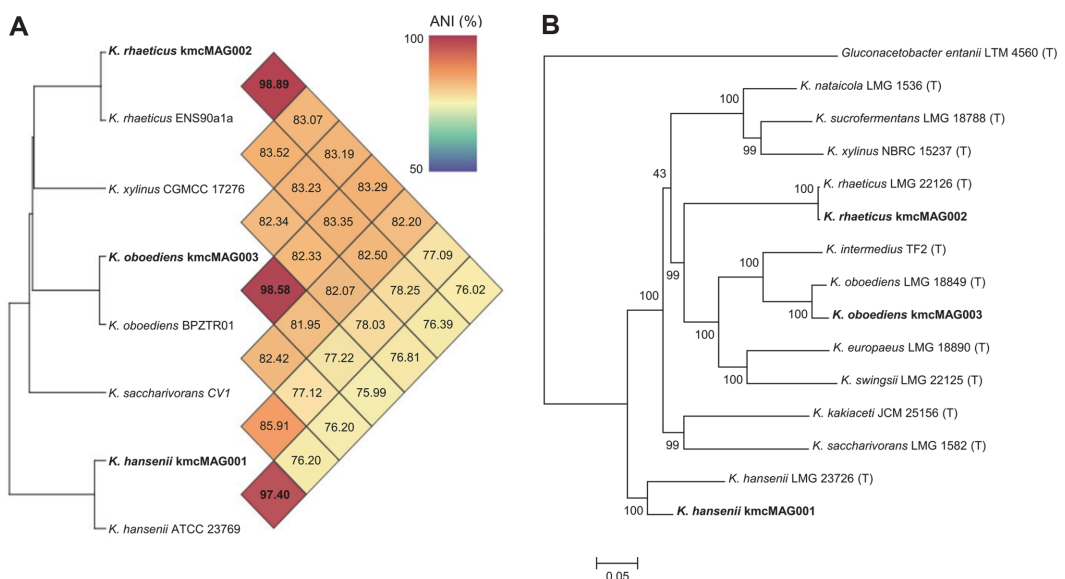


Fig. 4. Phylogenetic analysis between MAGs and related taxa. (A) The average nucleotide identity (ANI) values were calculated between reconstructed MAGs and the genomes of the closest strains selected by SCGs of Kaiju. (B) The Maximum-Likelihood phylogenetic tree of MAGs and genome sequences of the closest species (type strain). The phylogenetic tree was constructed using the PhaMe tool. Bootstrap analysis was performed by resampling 100 times the entire set, and the bootstrap values are displayed on the phylogeny tree.

Category	Functional feature	Description		
		(number of components)	(number of components)	(number of components)
Glycolysis		core module involving three-carbon compounds (6)		
Pyruvate oxidation		pyruvate \Rightarrow acetyl-CoA (4)		
Citrate cycle (TCA cycle)		TCA cycle, Krebs cycle (16)		
Citrate cycle (1st C oxidation)		oxaloacetate \Rightarrow 2-oxoglutarate (3)		
Citrate cycle (2nd C oxidation)		2-oxoglutarate \Rightarrow oxaloacetate (13)		
Peptose phosphate pathway (oxidation)		glucose 6P \Rightarrow ribulose 5P (4)		
Peptose phosphate pathway (non-oxidation)		fructose 6P \Rightarrow ribose 5P (6)		
PPPP biosynthesis		ribose 5P \Rightarrow PRPP (1)		
Entner-Doudoroff pathway		glucose-6P \Rightarrow glyceraldehyde-3P + pyruvate (5)		
Nucleotide sugar biosynthesis		glucose \Rightarrow UDP-glucose (3)		
URP-N-acetyl-D-glucosamine biosynthesis (prokaryotes)		glucose \Rightarrow UDP-GlcNAc (6)		
Reductive pentose phosphate cycle		glyceraldehyde-3P \Rightarrow ribulose-5P (5)		
PRPP (C-1-assoc)an acid metabolism		ATP-prypridine phosphate < \Rightarrow > AMP+PEP+diphosphosphate (2)		
Phosphate acetyltransferase-acidite kinase pathway		acetyl-CoA \Rightarrow acetate (2)		
Assimilatory sulfate reduction		sulfite \Rightarrow HS (5)		
NADH-tetradonin oxidoreductase		NADH prokaryotes (5)		
Succinate dehydrogenase		Succinate dehydrogenase, prokaryotes (4)		
Cytochrome bc ₁ complex respiratory unit		Cytochrome bc complex respiratory unit (3)		
Cytochrome c oxidase, prokaryotes		Cytochrome c oxidase, prokaryotes (3)		
Cytochrome c (ubiquinol) oxidase		prokaryotes and chloroplasts (4)		
F-type ATPase		prokaryotes and chloroplasts (7)		
Fatty acid biosynthesis (elongation)		initiation (6)		
Phosphatidylcholine PC biosynthesis		elongation (5)		
Phosphatidylethanolamine PE biosynthesis		PE \Rightarrow PC (1)		
Inositol monophosphate biosynthesis		PA \Rightarrow PS \Rightarrow PE (3)		
Adenine ribonucleotide biosynthesis		PRPP \Rightarrow Guanine \Rightarrow IMP (12)		
Guanine ribonucleotide biosynthesis		IMP \Rightarrow ADP ATP (5)		
Pyrimidine ribonucleotide biosynthesis		IMP \Rightarrow GMP GTP (5)		
Pyrimidine degradation		UMP \Rightarrow UDPUTP, CDPOCTP (3)		
Serine biosynthesis		uracil \Rightarrow beta-alanine, thymine \Rightarrow 3-aminoisobutyrate (4)		
Beta-alanine biosynthesis		glycinate-3P \Rightarrow serine (3)		
Cysteine biosynthesis		aspartate \Rightarrow homoserine \Rightarrow threonine (5)		
Vallinolactone biosynthesis		choline \Rightarrow betaine (2)		
Isoleucine biosynthesis		serine \Rightarrow cysteine (2)		
Leucine biosynthesis		pyruvate \Rightarrow valine (2)		
Lysine biosynthesis, succinyl-DAP pathway		threonine \Rightarrow 2-oxobutanate \Rightarrow isoleucine (5)		
Ornithine biosynthesis		2-oxocovalerate \Rightarrow 2-oxobutanate \Rightarrow isoleucine (6)		
Arginine biosynthesis		aspartate \Rightarrow 2-oxosuccinate (4)		
Phenylalanine biosynthesis		aspartate \Rightarrow tyrosine (7)		
Phytolamine biosynthesis		glutamate \Rightarrow ornithine (4)		
Histidine biosynthesis		ornithine \Rightarrow arginine (3)		
Shikimate pathway		glutamate \Rightarrow proline (3)		
Tryptophan biosynthesis		nicotinate \Rightarrow fumurate (7)		
Glutathione biosynthesis		arginine \Rightarrow ornithine \Rightarrow proline (3)		
NAD biosynthesis		PRPP \Rightarrow histidine (10)		
Coenzyme A biosynthesis		phosphoenolpyruvate + erythrose-4P \Rightarrow chorismate (6)		
Molybdenum cofactor biosynthesis		chorismate \Rightarrow tryptophan (7)		
Cobalamin biosynthesis		glutamate \Rightarrow glutathione (2)		
ATP-L-ribamose biosynthesis		aspartate \Rightarrow quinolinate \Rightarrow NAD (6)		
Sulfate assimilation		nicotinate \Rightarrow fumurate (7)		
Cellobiose biosynthesis bcs operon		arginine \Rightarrow ornithine \Rightarrow proline (3)		
Type II toxin-antitoxin system		PRPP \Rightarrow molybdenum cofactor (5)		
autotransp. peptidase		cobyrinate a, c-diGMP \Rightarrow cobalamin (8)		
autotransp. peptidase		dTDP- β -mannose biosynthesis (4)		
modulated cell killing regulon		Sulfate/sulfur assimilation (4)		
CSP-modulated cell killing regulon		beta1, rcsB		
Regulator of acylhomoserine lactone		marE, marF		
Quorum Sensing		trc		
		trBD		
		craA		
		auvA		
		Total	47	53
			53	53

Fig. 5. Comparison of the genomes among three *Komagataeibacter MAGs*. A total of 59 functional elements, including 53 pathways and 6 operons, were detected. Venn diagram shows the number of sharing genetic elements among MAGs. The annotation was conducted in module-based pathway and prediction of the operons using GhostKoala in the KEGG database and Prokka, respectively. Red bar indicates the presence of gene contents and blue bar indicates the absence of gene contents in each MAG. The elements varying in presence or absence are highlighted in red text.

identified in our three MAGs. Forty-one elements were commonly detected in all the MAGs. Five elements, bacterial pyruvate phosphate dikinase (PPDK) related pathway, betaine biosynthesis, polyamine biosynthesis, type II toxin-antitoxin system, and auto-repress quorum-regulated promoter *TraC* were unique in the *K. hansenii* MAG (kmcMAG001). Functional genetic elements of the *K. rhaeticus* (kmcMAG002) were similar to those in *K. oboediens* (kmcMAG003). One operon (*bcs*: biosynthesis of the bacterial cellulose) and ten genetic elements (nucleotide sugar biosynthesis, cytochrome o ubiquinol oxidase, inosine monophosphate biosynthesis, pyrimidine ribonucleotide biosynthesis, pyrimidine degradation, serine biosynthesis, ornithine biosynthesis coenzyme A biosynthesis, auto-repress quorum-regulated promoter *TraD*) were commonly detected in *K. rhaeticus* and *K. oboediens* MAGs. The sulfate-sulfur assimilation pathway was unique in the *K. oboediens* (kmcMAG003). Several important operons for the communication between microorganisms were detected in these *Komagataeibacter* MAGs. The competence-simulating peptide (CPS)-modulated cell killing regulon (*cinA*) and regulator of acylhomoserine lactone (*aiiA*), which are components of quorum sensing (QS) related operons, were detected in the three *Komagataeibacter* MAGs. Autorepressive quorum-regulated promoter of the *tra* gene was commonly detected in three MAGs. However, the *traC* was detected only in the kmcMAG001, and the *traD* was in the kmcMAG002 and kmcMAG003. The toxin-antitoxin (TA) system, represented with the type II TA *mazEF* operon, was unique in kmcMAG001.

Discussion

Although the diversity of KMCs showed fluctuation throughout the samples, the genus *Komagataeibacter* were still regarded as dominant organism of the KMC samples. As the genus *Komagataeibacter* was revealed as a key microorganism in our previous study [9], the analysis to investigate of genetic insight of *Komagataeibacter* is crucial for revealing the core function of KMC microbiomes in stressful environment. Therefore, we analyzed the alteration of functional gene features and reconstructed MAGs from whole metagenome sequences in KMC samples exposed to Mars-like conditions. We compared genetic elements in *Komagataeibacter* MAGs, which was dominant members in all the KMC samples, to understand the tolerance and reactivation of *Komagataeibacter* after exposure to Martian environments. Our results showed that genetic elements in *Komagataeibacter* species had the potential to survive and modulate the other microorganisms in KMC.

The profiles of functional genes in KMC samples were shifted after exposure to Mars-like conditions consist of 95.55% CO₂, 2.7% N₂, 1.6% Ar, 0.15% O₂, ~370 ppm H₂O and a pressure of 980 Pa [9, 10]. Functional genes in the microbiome of readapted samples (KMC_c) were more different to those of control samples (KMC_4 and KMC_5) than post-flight reactivated samples (KMC_b). These differences of functional features were caused by the alteration of microbiota according to conditions after exposure to space environment. The exposure to Mars-like condition affected the microbiome in KMCs and re-cultured microbiota after exposure was different to the microbiota in non-exposed controls (laboratory-kept samples). The shifted microbiota in KMCs and functional genes were also different according to exposed layer in carrier outside the ISS. The functional genes in the microbiome of top-layer samples (KMC_1) were more different to those of control samples than middle and bottom-layer samples (KMC_2 and KMC_3) in both reactivated and readapted samples. The top-layer sample was exposed to UV radiation which could emit about 4.92×10^2 kJ / m² and 0.5 Gray (Gy) of cosmic-ionizing radiation, and the samples of middle and bottom layer were maintained unilluminated and UV-protected condition. Therefore, the microbiome in top-layer samples was exposed to strong stressors and their influences were higher than those in other-layer samples. *K. hansenii* was still dominant in reactivated (cultured post-flight samples for 2 weeks) samples. In particular, the proportion of this species was the highest in reactivated sample of top-layer exposure (KMC_1b). *K. oboediens* was dominated in readapted samples (sub-cultured for 2.5-year). The microbiota in middle-layer samples were similar between reactivated and readapted conditions. The proportion of unclassified taxa was decreased in KMCs after exposure to harsh conditions. This indicates that *K. hansenii* was tolerant to harsh condition including UV exposure and could reactivate immediately after return in reactivated samples. However, *K. oboediens* was gradually dominated in repeated cultures for relatively long period (2.5-year). Although the microbiome in KMC was influenced by exposure to Mars-like condition, *Komagataeibacter* spp. survived and dominated in reactivated and readapted samples. In addition, three *Komagataeibacter* MAGs were obtained from whole metagenome sequences with high quality (completeness > 90% and contamination < 5%). We analyzed and compared genomic elements among reconstructed *Komagataeibacter* MAGs in KMC samples.

Two *Komagataeibacter* species were dominant in short-read based result, whereas three *Komagataeibacter* species were obtained in MAGs based result. This difference could be due to the analysis method including assembly and reference databases. In addition, genomic contents in *K. rhaeticus* MAG were similar to those in *K. oboediens*. Thus, it is possible that functional genetic elements of *K. rhaeticus* were identified as gene contents of *K. oboediens* in short-read based analysis. Forty-one genetic elements were common among three *Komagataeibacter* MAGs. Three MAGs contained QS operons, which are essential for making the microbiome act like a multicellular single organism [28]. The QS system could play a role in the communication between microorganisms within KMC samples in harsh conditions, including UV radiation, high amount CO₂, lack of water resource, and limitation of nutrient availability [29, 30]. Therefore, the QS system could be one of the driving factors for microbial survival in KMC samples.

Five unique genetic elements in *K. hansenii* could provide clue for tolerance to harsh environment at top-layer KMC sample. The type II TA system has been reported as an important system for stabilizing microbial community in stressed environment [31, 32]. Microorganisms in KMC sample could be diminished during long-term experiments by strong external stressors, and survival members had the advantage for growth, including space and nutrients supply in the limited environment by programmed cell death mediated by the TA system. The

PPDK pathway is a CAM-light pathway that occurs in the cytosol with the proton gradient for ATP production occurring across the bacterial cytoplasmic membrane [33]. Microbiota in KMC samples can survive by using the PPDK pathway, which can be activated alternative carbohydrate fixation under high CO₂ condition and dry environment with low oxygen concentration similar to Mars-like environment [34, 35]. The enzymes in the betaine biosynthesis pathway act in the biosynthesis of glycine betaine from choline. The glycine betaine is an efficient osmotic solute found in a wide range of bacteria, and this compound accumulates in response to osmotic stress as an osmoprotectant. Osmotic stress is one of the major stress factors in KMC outside the ISS as well as UV radiation, the glycine betaine is possible to protect KMCs against Mars-like environmental stress [36, 37]. In addition, glycine betaine could be a vigorous protectant against mutagenic sources such as radiation-induced damage [38]. The polyamines are organic alkaline compounds having multiple amino groups with a net positive charge at physiological pH. Because of their unique charge-structure, polyamines play a crucial role in the maintenance of negatively charged nucleic acids and are essential for normal cellular growth and multiplication [39]. Some polyamines, such as putrescine, modulate numerous cellular processes, including transcription and translation [40]. The predicted polyamine biosynthesis pathway in *K. hansenii* kmcMAG001 could produce putrescine by ornithine decarboxylase or arginine decarboxylase. Although further understanding of the mechanisms is necessary, the synthesis of polyamines could be an important factor for microbiome stabilization. These functional gene elements of *K. hansenii* MAG could be a clue for tolerance for harsh condition and protection other microbes in KMCs exposed to Mars-like conditions with a low level of water and UV radiating environments.

The unique genetic content of *K. oboediens* kmcMAG003 was the sulfate-sulfur assimilation pathway. Sulfur is an essential element in several metabolisms, including the amino acids methionine and cysteine, vitamin B7 (biotin), and glutathione [41, 42]. Therefore, the sulfate-sulfur assimilation pathway of *K. oboediens* could supply sulfur resource to microbes in KMCs. However, this unique pathway could not fully explain why *K. oboediens* had achieved more successful flourish in nutrient-rich and mild conditions than *K. hansenii* during re-adaptation. *K. oboediens* has eleven more functional elements than *K. hansenii*. This indicates that *K. oboediens* could be more functionally complex organism than *K. hansenii*. Competitive relationship between two species could not be applied in this case, because the relative abundance of *K. hansenii* was maintained and it was dominant in middle and bottom-layer samples. Therefore, *K. hansenii* in top-layer KMC sample was tolerated to harsh condition and could be reactivated immediately after return from ISS. However, strong stressors were influenced on *K. hansenii* at top-layer and this species could not flourish during readaptation.

In conclusion, the microbiome in KMCs exposed to Mars-like conditions was changed, but the dominant *Komagataebacter* spp. especially *K. hansenii*, *K. rhaeticus*, and *K. oboediens* tolerated and could protect other microbes in KMC by retaining their genetic properties and active specific pathways. *K. oboediens* is the dominant member in KMC exposure to space condition during repeated cultivation. Our results can extend the understanding the microbiome in Kombucha exposed to extra-terrestrial conditions towards developing a KMC with minimal microbial composition.

Acknowledgments

This research was supported by the Bio & Medical Technology Development Program of the National Research Foundation of Korea (NRF) funded by the Ministry of Science and ICT (2021M3A9I4023974), Basic Science Research Program through the NRF of Korea funded by the Ministry of Education (2021R1A6A1A03044501), and the Korea Health Technology R&D Project through the Korea Health Industry Development Institute (KHIDI) funded by the Ministry of Health & Welfare (HP20C0082). K.J.A. acknowledges the Taif University Researchers Supporting Program (project number: TURSP-2020/128), Taif University, Saudi Arabia.

Conflict of Interest

The authors have no financial conflicts of interest to declare.

References

- Dufresne C, Farnworth E. 2000. Tea, Kombucha, and health: a review. *Food Res. Int.* **33**: 409-421.
- Greenwalt C, Steinkraus K, Ledford R. 2000. Kombucha, the fermented tea: microbiology, composition, and claimed health effects. *J. Food Prot.* **63**: 976-981.
- Jayabalan R, Malbaša RV, Lončar ES, Vitas JS, Sathishkumar M. 2014. A review on kombucha tea - microbiology, composition, fermentation, beneficial effects, toxicity, and tea fungus. *Compr. Rev. Food Sci. Food Saf.* **13**: 538-550.
- Arikan M, Mitchell AL, Finn RD, Gürel F. 2020. Microbial composition of Kombucha determined using amplicon sequencing and shotgun metagenomics. *J. Food Sci.* **85**: 455-464.
- Villarreal-Soto SA, Bouajila J, Pace M, Leech J, Cotter PD, Souchard J-P, et al. 2020. Metabolome-microbiome signatures in the fermented beverage, Kombucha. *Int. J. Food Microbiol.* **333**: 108778.
- Gomes RJ, Borges MdF, Rosa MdF, Castro-Gómez RJH, Spinos WA. 2018. Acetic acid bacteria in the food industry: systematics, characteristics and applications. *Food Technol. Biotechnol.* **56**: 139-151.
- Ramachandran S, Fontanille P, Pandey A, Larroche C. 2006. Gluconic acid: properties, applications and microbial production. *Food Technol. Biotechnol.* **44**: 185-195.
- Banerjee S, Schlaeppi K, van der Heijden MG. 2018. Keystone taxa as drivers of microbiome structure and functioning. *Nat. Rev. Microbiol.* **16**: 567-576.
- Góes-Neto A, Kukharenko O, Orlovska I, Podolich O, Imchen M, Kumavath R, et al. 2021. Shotgun metagenomic analysis of kombucha mutualistic community exposed to mars-like environment outside the international space station. *Environ. Microbiol.* **23**: 3727-3742.

10. Podolich O, Kukharenko O, Haidak A, Zaets I, Zaika L, Storozhuk O, et al. 2019. Multimicrobial kombucha culture tolerates mars-like conditions simulated on low earth orbit. *Astrobiology* **19**: 183-196.
11. Beghini F, McIver LJ, Blanco-Míguez A, Dubois L, Asnicar F, Maharjan S, et al. 2021. Integrating taxonomic, functional, and strain-level profiling of diverse microbial communities with bioBakery 3. *Elife* **10**: e65088.
12. Kruskal JB. 1964. Nonmetric multidimensional scaling: a numerical method. *Psychometrika* **29**: 115-129.
13. Bray JR, Curtis JT. 1957. An ordination of the upland forest communities of southern Wisconsin. *Ecol. Monogr.* **27**: 326-349.
14. Dixon P. 2003. VEGAN, a package of R functions for community ecology. *J. Veg. Sci.* **14**: 927-930.
15. Li D, Liu C-M, Luo R, Sadakane K, Lam T-W. 2015. MEGAHIT: an ultra-fast single-node solution for large and complex metagenomics assembly via succinct de Bruijn graph. *Bioinformatics* **31**: 1674-1676.
16. Langmead B, Salzberg SL. 2012. Fast gapped-read alignment with Bowtie 2. *Nat. Methods* **9**: 357-359.
17. Menzel P, Ng KL, Krogh A. 2016. Fast and sensitive taxonomic classification for metagenomics with Kaiju. *Nat. Commun.* **7**: 11257.
18. Eren AM, Esen ÖC, Quince C, Vineis JH, Morrison HG, Sogin ML, et al. 2015. Anvi'o: an advanced analysis and visualization platform for 'omics data. *PeerJ* **3**: e1319.
19. Parks DH, Imelfort M, Skennerton CT, Hugenholtz P, Tyson GW. 2015. CheckM: assessing the quality of microbial genomes recovered from isolates, single cells, and metagenomes. *Genome Res.* **25**: 1043-1055.
20. Camacho C, Coulouris G, Avagyan V, Ma N, Papadopoulos J, Bealer K, et al. 2009. BLAST+: architecture and applications. *BMC Bioinformatics* **10**: 421.
21. Sayers EW, Agarwala R, Bolton EE, Brister JR, Canese K, Clark K, et al. 2019. Database resources of the national center for biotechnology information. *Nucleic Acids Res.* **47**: D23-D28.
22. Lee I, Kim YO, Park S-C, Chun J. 2016. OrthoANI: an improved algorithm and software for calculating average nucleotide identity. *Int. J. Syst. Evol. Microbiol.* **66**: 1100-1103.
23. Shakya M, Ahmed SA, Davenport KW, Flynn MC, Lo C-C, Chain PS. 2020. Standardized phylogenetic and molecular evolutionary analysis applied to species across the microbial tree of life. *Sci. Rep.* **10**: 1723.
24. Kanehisa M, Sato Y, Morishima K. 2016. BlastKOALA and GhostKOALA: KEGG tools for functional characterization of genome and metagenome sequences. *J. Mol. Biol.* **428**: 726-731.
25. Seemann T. 2014. Prokka: rapid prokaryotic genome annotation. *Bioinformatics* **30**: 2068-2069.
26. Papudeshi B, Haggerty JM, Doane M, Morris MM, Walsh K, Beattie DT, et al. 2017. Optimizing and evaluating the reconstruction of Metagenome-assembled microbial genomes. *BMC Genomics* **18**: 915.
27. Lee I, Barh D, Podolich O, Brenig B, Tiwari S, Azevedo V, et al. 2021. Metagenome-assembled genome sequences obtained from a reactivated Kombucha microbial community exposed to a Mars-like environment outside the International Space Station. *Microbiol. Resour. Announc.* **10**: e00549-00521.
28. Ng W-L, Bassler BL. 2009. Bacterial quorum-sensing network architectures. *Annu. Rev. Genet.* **43**: 197-222.
29. Rutherford ST, Bassler BL. 2012. Bacterial quorum sensing: its role in virulence and possibilities for its control. *Cold Spring Harb. Perspect. Med.* **2**: a012427.
30. Solano C, Echeverz M, Lasa I. 2014. Biofilm dispersion and quorum sensing. *Curr. Opin. Microbiol.* **18**: 96-104.
31. Erental A, Sharon I, Engelberg-Kulka H. 2012. Two programmed cell death systems in *Escherichia coli*: an apoptotic-like death is inhibited by the mazEF-mediated death pathway. *PLoS Biol.* **10**: e1001281.
32. Yamaguchi Y, Park J-H, Inouye M. 2011. Toxin-antitoxin systems in bacteria and archaea. *Annu. Rev. Genet.* **45**: 61-79.
33. Zhang S, Bryant DA. 2011. The tricarboxylic acid cycle in cyanobacteria. *Science* **334**: 1551-1553.
34. Cushman JC, Bohnert HJ. 1999. Crassulacean acid metabolism: molecular genetics. *Annu. Rev. Plant Biol.* **50**: 305-332.
35. Osmond C. 1978. Crassulacean acid metabolism: a curiosity in context. *Annu. Rev. Plant Physiol.* **29**: 379-414.
36. Kerovuo J, Reiniikainen T, Nyysönen A, Kaukinen P, von Weymarn N. 2000. Extreme halophiles synthesize betaine from glycine by methylation. *J. Biol. Chem.* **275**: 22196-22201.
37. Monobe M, Uzawa A, Hino M, Ando K, Kojima S. 2005. Glycine betaine, a beer component, protects radiation-induced injury. *J. Radiat. Res.* **46**: 117-121.
38. Smith LT, Pocard J-A, Bernard T, Le Rudulier D. 1988. Osmotic control of glycine betaine biosynthesis and degradation in *Rhizobium meliloti*. *J. Bacteriol.* **170**: 3142-3149.
39. Shah P, Swiatlo E. 2008. A multifaceted role for polyamines in bacterial pathogens. *Mol. Microbiol.* **68**: 4-16.
40. Schneider J, Wendisch VF. 2011. Biotechnological production of polyamines by bacteria: recent achievements and future perspectives. *Appl. Microbiol. Biotechnol.* **91**: 17-30.
41. Kawano Y, Suzuki K, Ohtsu I. 2018. Current understanding of sulfur assimilation metabolism to biosynthesize L-cysteine and recent progress of its fermentative overproduction in microorganisms. *Appl. Microbiol. Biotechnol.* **102**: 8203-8211.
42. Mendoza-Cózatl D, Loza-Távara H, Hernández-Navarro A, Moreno-Sánchez R. 2005. Sulfur assimilation and glutathione metabolism under cadmium stress in yeast, protists and plants. *FEMS Microbiol. Rev.* **29**: 653-671.